-RESEARCH PAPER-

International Journal of Mining and Geo-Engineering IJMGE

IJMGE 60-1 (2026) 105-112 DOI: 10.22059/IJMGE.2026.400194.595289

Modification of the Kuz-Ram model using response surface methodology to optimise blast fragmentation

Onalethata Saubi [a, *] and Raymond S. Suglo [a]

[a] *Department of Mining Engineering, Botswana International University of Science and Technology, Palapye, Botswana.*

Article History:

Received: 06 August 2025.
Revised: 27 October 2025.
Accepted: 26 March 2026.

ABSTRACT

Predicting and optimising blast-induced rock fragmentation is essential for improving downstream mining operations such as loading, hauling, and comminution. The widely used Kuz-Ram model often requires heuristic calibration of the rock factor, which limits its predictive accuracy in heterogeneous rock masses. This study introduces a modified Kuz-Ram model that integrates response surface methodology (RSM) to refine the rock factor estimation based on the blastability index (BI). A dataset of 80 production blasts from Orapa Diamond Mine, Botswana, incorporating four input parameters, powder factor, charge, rock factor, and blastability index was analysed. The RSM-modified model demonstrated a 12.2% improvement in prediction accuracy compared to the traditional Kuz-Ram model, achieving an R^2 of 0.579, with RMSE and MAE reduced to 5.71 and 3.07 respectively. The approach preserves the empirical simplicity of Kuz-Ram while explicitly modelling nonlinear parameter interactions, offering a transparent yet robust tool for blast design. This method is practical for mines requiring rapid calibration to site-specific geological conditions and can be extended to include additional parameters, such as delay timing, in future work.

Keywords: *Kuz-Ram model, Response surface methodology, Blastability index, Rock factor, Optimising blast fragmentation.*

1. Introduction

Efficient rock breakage through blasting remains a crucial task in surface mining. Fragment size distribution dictates the subsequent steps in the mining value chain such as loading, hauling, and comminution and thus directly affects operational costs and productivity [1-3]. Blast-induced fragmentation refers to the post-blast size distribution of the rock mass, encompassing the range of fragment sizes produced by blasting activities. Achieving an optimal fragmentation is essential, as both excessive fines and oversized boulders can lead to inefficiencies in materials handling and processing [4-5]. In addition to fragmentation control, safety considerations such as flyrock and ground vibration remain critical, optimising blast design must therefore account for both efficiency and safety outcomes [6]. The mean fragment (X_{50}) size represents the average particle size of the blasted material, providing an overall measure of fragmentation. It is a valuable parameter for assessing blast performance, as it helps in evaluating the uniformity of rock breakage and optimising downstream processes and minimising energy consumption [7-8].

Kuznetsov [9] introduced a formula that establishes a relationship between rock mass, the amount of explosive used (specific charge), and the average fragment size.

$$X_{50} = Rf \times K^{-4/5} \times Q^{1/6} \tag{1}$$

where X_{50} is the mean fragment size (cm), Rf is the rock factor, K is the powder factor in kg per cubic metre, Q is mass in kg of the nitroglycerine-based explosive used per hole.

Because nitroglycerine-based explosives are known to have high velocities of detonation, the mean fragment size in equation 1 applies to them. However, equation 1 can be modified into equation 2 to take into account the widely used explosive ANFO, which is less potent than nitroglycerine-based explosives:

$$X_{50} = \mathrm{Rf} \times \mathrm{K}^{-4/5} \times \mathrm{Q}^{1/6} \times \left(\frac{115}{\mathrm{RWS}}\right)^{19/20} \tag{2}$$

where RWS is the relative weight strength of the explosive compared to ANFO.

Developed by Cunningham [10], the Kuz-Ram model combines Kuznetsov's characteristic size equation with a Rosin-Rammler distribution for fragment size. Key inputs include explosive properties, powder factor and a rock factor meant to capture the geomechanical characteristics of the rock. Although popular, the model often requires recalibration of the rock factor, especially for non-homogeneous rock masses [11-12]. Consequently, the model's applicability may be constrained when site-specific geology or blast designs deviate from the original calibration conditions of the rock factor and distribution coefficients [13]. Previous research has demonstrated that blast-induced effects such as vibration and flyrock can be effectively modelled and minimised through optimisation of blast parameters, highlighting the importance of integrating geological and design factors in predictive frameworks [14].

Several researchers have proposed modifications to the Kuz-Ram model to improve its applicability across varying geological conditions. Cunningham [15] revised the model constants and incorporated blast geometry considerations for broader field use, while Cunningham [16] further refined these calibrations to address large-scale open-pit operations. More recent studies have explored simulation-based and hybrid optimisation techniques to improve blasting outcomes, achieving higher precision in predicting fragmentation and reducing downstream processing costs [17]. Prior to computing the characteristic fragment size in the Kuz-Ram model, the rock factor must be established. The

* Corresponding author: *E-mail address:* : so13000604@biust.ac.bw (O. Saubi).

rock factor is obtained by multiplying the characteristics of the rock mass by a coefficient called the land coefficient. In homogeneous rock masses with few discontinuities, a value for the land coefficient suggested by Lilly [11] has been found to yield accurate predictions. However, when used on heterogeneous rock formations, its accuracy decreases [12]. To improve fragmentation size forecasts, Gheibie et al. [18] proposed a land coefficient that is comparable to Lilly's. Tosun et al. [12] established a linear association between the predictions of the Kuz-Ram model and the outcomes of image analysis by introducing a modified land coefficient specifically designed for limestone deposits in Turkey. However, the management of the constant in the linear correlation equation was not specified in their work. The blastability index (BI) was introduced by Lilly [11], which laid the groundwork for further improvements, emphasizing that a comprehensive understanding of the rock's mechanical and physical characteristics, as well as its structural geology, should also be considered. In later work, Cunningham [15] proposed the A-factor classification within the Kuz-Ram framework, which is conceptually related but distinct from BI.

Recent updates to BI extend beyond Lilly's original formulation. Contemporary reviews highlight trends toward data-driven and 3-D assessments of blastability, the integration of digital mapping, and intelligent parameter acquisition to reduce subjectivity in ratings [19]. For joint-rich masses with very close spacing, the blastability quality system (BQS) provides an alternative classification tuned to discontinuity density and orientation [20]. Other studies relate BI (or BI-proxies) to drill monitoring features and machine learning estimators to enable continuous spatial prediction and mine-to-mill control [21]. These developments are compatible with our approach because the response surface methodology-modified Kuz-Ram only requires a scalar blastability descriptor; any updated BI (or equivalent index) can replace Lilly's term without altering the modelling workflow.

The geological features of the rock mass have a major impact on how well blasting operations work. The blastability index (BI) is used to measure how easily the rock can be fragmented by blasting. To assess the rock's vulnerability to blasting, the BI incorporates a number of rock mass characteristics, such as uniaxial compressive strength, rock density, joint spacing, joint orientation, and the rock mass description [19]. A higher BI indicates rock that is more amenable to efficient fragmentation, thereby optimising blasting outcomes and enhancing downstream processes such as loading, hauling and crushing. Implementing the BI in blast design allows for tailored explosive energy distribution, minimising overbreak and reducing operational costs. Studies have demonstrated the utility of the BI in improving wall control and overall blast performance in hard rock mining environments [11, 18, 22].

In a study, Lawal [13] addressed the tendency of the traditional Kuz-Ram model to overestimate rock fragment sizes. He proposed a modified version that recalibrates the rock factor using image analysis data and the least squares method. This adjustment reduced prediction errors from over 60% to about 3.5%, offering a more accurate and cost-effective method for estimating fragment sizes in mining operations. Some researchers have employed machine learning methods such as artificial neural networks, support vector regression, tree-based ensembles and hybrid algorithms to predict fragmentation [23-30]. While capable of high predictive accuracy, these methods can be demanding in data size and curation [31]. Moreover, the opaque nature of machine learning solutions poses challenges for engineering interpretation (black box solutions) and regulatory acceptance [32].

While previous studies have modified the Kuz-Ram model to enhance its predictive accuracy for specific conditions, they remained largely heuristic or linear, relying on empirical adjustments without fully capturing nonlinear interactions among rock properties and blast parameters. In particular, limited work has explicitly modelled the nonlinear relationship between blastability index (BI) and rock factor, despite BI's recognised influence on fragmentation outcomes. This gap motivated the present study to integrate response surface methodology (RSM) into the Kuz-Ram framework, enabling systematic modelling of nonlinear effects and providing a more adaptable and transparent predictive tool for heterogeneous rock masses. To address the limitations inherent in the Kuz-Ram model, particularly its sensitivity to variations in rock mass properties, this study integrates RSM to enhance predictive accuracy. Using second-order polynomials, the RSM is a statistical method that models nonlinear interactions [33]. Compared to other empirical modifications, RSM offers superior flexibility, interpretability, and data efficiency, making it a viable alternative to black-box machine learning models.

Unlike traditional regression models, which may struggle to capture complex interactions between blast parameters, RSM provides a structured approach to explore nonlinear relationships through response surfaces [34]. Additionally, empirical models that rely solely on heuristic adjustments may lack adaptability to varying site conditions. The RSM strikes a balance by allowing for mathematical rigour in model development while maintaining transparency and ease of implementation [35]. Its ability to generate explicit polynomial equations enables straightforward optimisation of blast parameters, making it a practical choice for improving fragmentation prediction in mining operations.

This study introduces a novel refinement of the Kuz-Ram model by applying RSM to explicitly capture the nonlinear relationship between blastability index and rock factor. Unlike previous heuristic or linear modifications, the proposed approach improves predictive accuracy by 12.2% while maintaining empirical simplicity, making it practical for site-specific calibration in operational mining conditions. This work demonstrates the successful integration of RSM into the Kuz-Ram framework, bridging the gap between traditional empirical models and complex black-box machine learning methods.

1.1. Mine case study

The largest open pit diamond mine in the world by area is the Orapa Diamond Mine, which is situated in Botswana's Central District. It is located in the village of Orapa, some 240 km west of Francistown. Debswana, a joint venture between De Beers and the Botswana government, is the owner of the mine. The geology of the area comprises Karoo Supergroup, which includes both volcanic and sedimentary formations and the Orapa kimberlite rock, which was discovered in 1967 by a group of De Beers geologists. This geological sequence contains basalt lavas that are Stormberg-aged and sits on top of Archaean granite. The Orapa kimberlite pipe has an ovoid surface exposure that is roughly 1,500 m long and 1,000 m wide. The kimberlite rocks were formed about 93 million years ago during the late Cretaceous period [36].

Blasting operations at Orapa use 400 g pentolite boosters and electronic detonators (15 m and 20 m). The explosive used is Power Gel S135B emulsion with relative weight strength of 115% and density of 1250.51 kg/m³, which is pumped into blast holes from a mobile manufacturing unit via a hose pipe, following the charge sheet specifications: 16 kg/m for 127 mm diameter holes, 27 kg/m for 165 mm diameter holes, and 61.4 kg/m for 250 mm diameter holes. A stemming depth of 5 m per blast hole is required, with a tolerance of ±0.3 m. Tailings are used as stemming material for ore blasts, while crushed waste rock is used for stemming the blastholes in waste zones.

Currently, mining operations at Orapa extend to a depth of approximately 305 m, with plans to reach 350 m by 2026. The average bench height is 15 m, with 40 to 60 holes per row and 15 to 25 rows per blast. The mine operates seven days a week, extracting 20 million tonnes of ore and an additional 40 million tonnes of waste rock annually. Orapa produces about 10.8 million carats of diamonds per year, with a recoverable ore grade of about 0.87 carats per tonne. Figure 1 shows the location of the Orapa Diamond Mine along with a satellite image of the site.

2. Materials and methods

A dataset comprising 80 blasting events (See Table 1) was collected from the blasting operations at Debswana Orapa Diamond Mine. Each record contained detailed blast design parameters, explosive characteristics, and geomechanical properties of the kimberlite rock mass. Prior to analysis, the dataset underwent data cleaning to remove

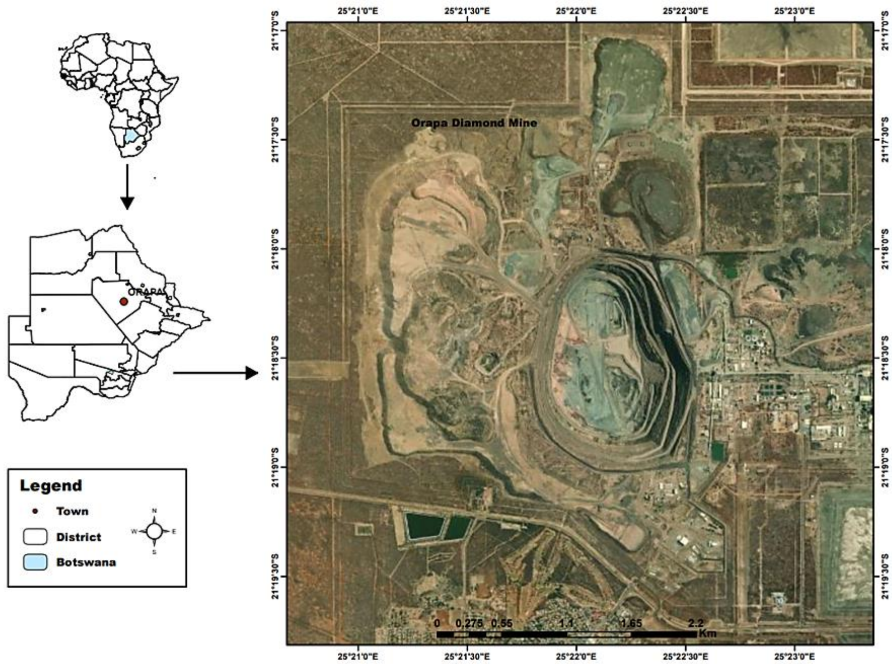

Figure 1: Location of orapa diamond mine.

incomplete records, correct unit inconsistencies, and verify the accuracy of field measurements. Outliers were assessed based on operational limits (e.g., abnormal powder factor or charge values) and cross-checked with mine production logs to ensure data integrity. For each blast, fragmentation results (mean fragment size, X_{50}) were obtained through image analysis of post-blast muckpiles using Split-Desktop software. Photographs were captured under controlled lighting conditions and scaled using reference objects to minimise measurement errors. Across 80 production blasts, we targeted up to five muckpile photographs per blast. After standard quality control (QC) (focus, lighting/occlusion, and scale visibility), 355 images were retained and analysed in Split-Desktop (n = 355). To avoid pseudo-replication, PSD metrics were summarised per blast (per-blast average of QC-passed images). Geomechanical data, including uniaxial compressive strength (UCS), joint spacing, and rock density, were recorded to calculate the Blastability Index (BI) using Lilly's empirical method.

This dataset provided four primary input parameters, charge (C), powder factor (Pf), rock factor (Rf), and blastability index (BI), and a single output parameter, mean fragment size (X_{50}), which were used for model development and validation. Statistical analyses, scatter plots, and response surface figures were generated using Python (Matplotlib, NumPy, and SciPy libraries), enabling quantitative evaluation of parameter interactions and model performance. Figure 2 shows the pairwise correlation analysis of input parameters, charge, powder factor, rock factor, blastability index, and mean fragmentation as the output. The scatter plots show the relationships between these variables, while the histograms illustrate their distributions.

A positive correlation between charge (C) and mean fragmentation (X_{50}) indicates that blasts with larger total charge tended to produce coarser mean sizes (larger X_{50}) in this dataset. By contrast, higher Pf (energy per unit rock volume) generally corresponds to smaller X_{50} (finer fragmentation), consistent with blasting principles [37-39]. However, variability in this relationship may result from geological factors such as jointing, weathering, and in-situ stresses. The relationship between powder factor and mean fragmentation shows modest scatter, indicating that while powder factor is a key driver, its effect is context-dependent on geology and blast design (e.g., burden, spacing, stemming).

Table 1. Descriptive statistics for the variables used in the study (n = 80).

Variable	Units	Minimum	Maximum	Mean	Std. Deviation
Charge	kg	549.8	617.2	589.4	17.4
Powder factor	kg/m³	0.647	0.800	0.705	0.035
Rock factor	-	5.68	9.17	7.84	0.75
Blastability index	-	27.7	60.1	43.2	8.2
Mean fragmentation	mm	50.1	98.2	80.4	9.3

By contrast, rock factor and mean fragmentation show a direct (positive) relationship: higher rock factor (more difficult-to-blast rock) is associated with larger X_{50} (coarser mean size) due to increased resistance to breakage. This underscores the need to optimise the charge-to-rock-strength ratio (e.g., via powder factor/charge concentration) as RF rises to maintain the desired size distribution. A positive relationship with relative dispersion between blastability index and mean fragmentation indicates that rock masses with higher blastability index values break more effectively, highlighting the importance of geological assessments, such as joint spacing and fracture density, in blast optimisation. Significant trends are often shown by interactions between independent variables. For example, higher charges are usually associated to higher blastability indices, indicating that blast efficiency increases in more blastable rock conditions. Furthermore, the scattered correlation between rock factor and powder factor emphasises the need to modify powder factor based on specific geological conditions.

These findings emphasise the need for an integrated approach to blast design where charge, powder factor, and rock properties are optimised at the same time. A positive correlation between blastability index and mean fragmentation highlights the importance of pre-blast rock mass characterisation, while the observed variability in powder factor vs. fragmentation shows the need for site-specific calibration over generalised blasting guidelines. Figure 3 is a correlation matrix which further quantifies the relationships between explosive charge, powder factor, rock factor, blastability index, and mean fragmentation. It shows a strong positive correlation (0.90) between rock factor and mean

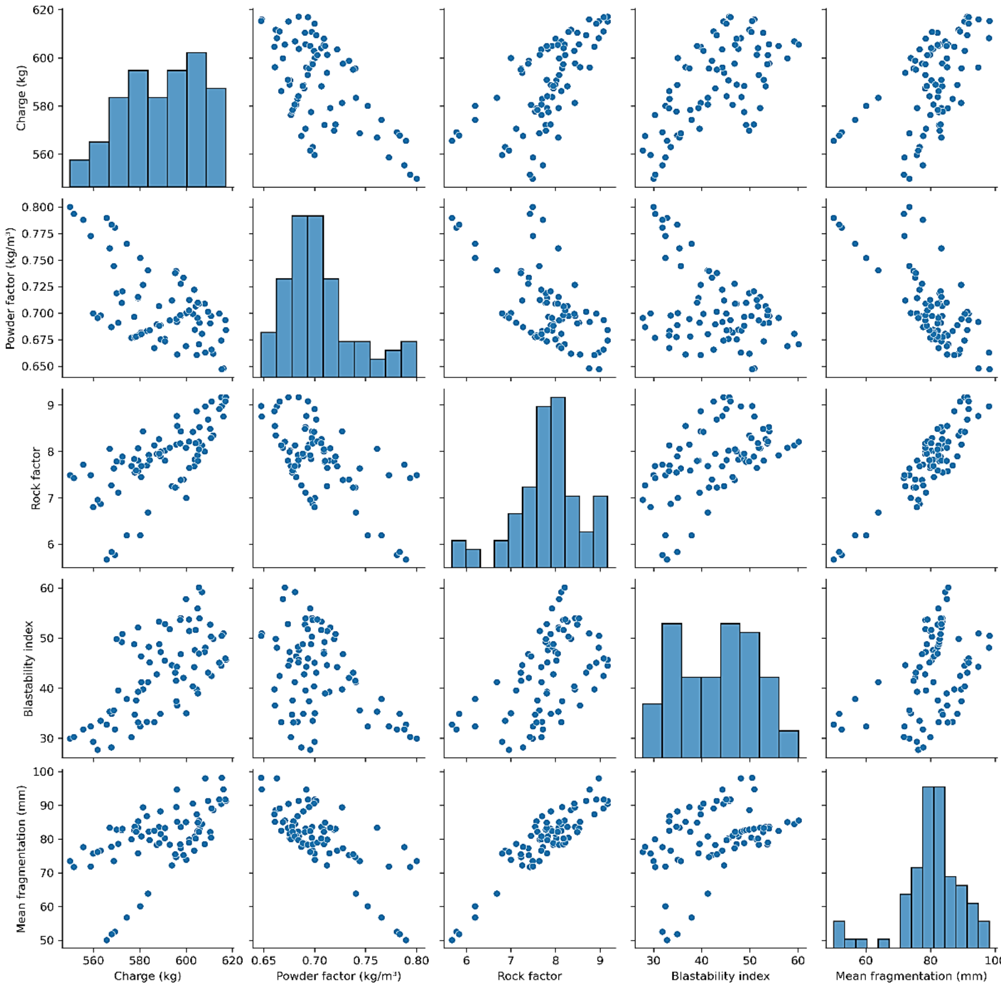

Figure 2. Pair wise relationship of the parameters.

fragmentation, supporting the previous finding that harder rock masses lead to coarser fragmentation due to their resistance to breakage. This suggests that rock factor is a dominant predictor of fragmentation and should be carefully considered in blast optimisation. The blastability index also exhibits a positive but low correlation (0.39) with mean fragmentation, validating its role as a key predictor in response surface modelling (RSM). It highlights the importance of incorporating geological assessments such as joint spacing and fracture density in blast design.

Also from Figure 3, there is a moderate correlation (0.55) between explosive charge and mean fragmentation, suggesting that while an increase in explosive charge enhances fragmentation, it is not the only determining factor. This supports the earlier observation that geological conditions influence how effectively explosive energy is utilised. The powder factor exhibits a strong negative correlation (-0.72) with mean fragmentation, consistent with theoretical predictions that a higher powder factor results in finer fragmentation [38]. However, as Figure 2 shows some scatter in this relationship, it implies that powder factor must be optimised in conjunction with burden, spacing, and type of stemming for site-specific calibration rather than relying on generic blasting guidelines.

Blastability index in Orapa mine is calculated based on the Lilly [11] relation as shown in equations 3 to 5. Table 2 summarises some of the blastability index parameters and their rating while Figure 4 shows the images of the muckpile that are processed with Split Desktop Software to generate the particle size distribution curve that is used to determine the mean fragmentation.

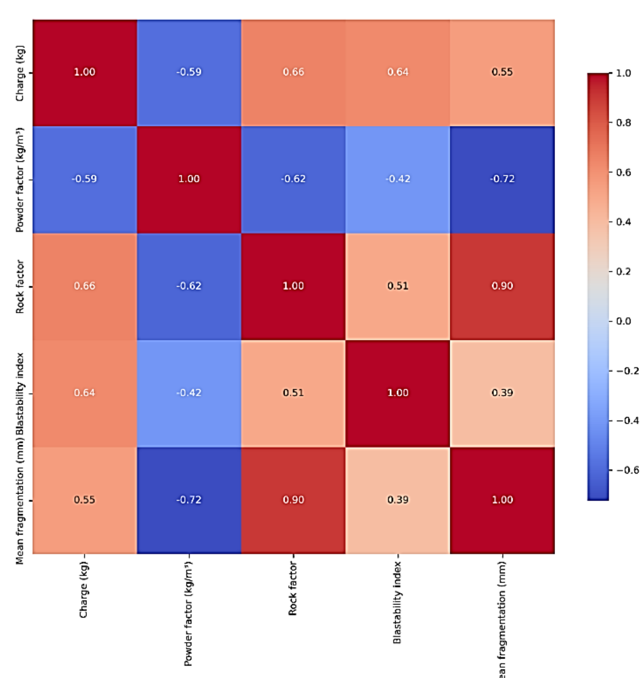

Figure 3. Correlation matrix of blasting parameters.

$$BI = 0.5(RMD + JPS + JPO + RDI + S) \quad (3)$$

$$S = 0.05 \times UCS \quad (4)$$

$$RDI = 25 \times \text{Rock density} - 50 \quad (5)$$

where *BI* is the blastability index, *RMD* is the rock mass description, *JPS* is the joint plane spacing, *JPO* is the joint plane orientation, *RDI* is the rock density influence, *S* is the rock strength influence, and *UCS* is the uniaxial compression strength of the rock.

Table 2. Blastability index parameters and their rating.

Parameters of Blastability Index	Rating
Rock Mass Description (RMD)	
Powdery/ Friable	10
Blocky	20
Massive	50
Joint Plane Spacing (JPS)	
Close (< 0.1)	10
Intermediate (0.1 - 1.0 m)	20
Wide (> 0.1m)	50
Joint Plane Orientation (JPO)	
Horizontal	10
Dip out of face	20
Strike normal to face	30
Dip in to face	40

Source (Lilly [10])

2.1. Response surface model formulation

RSM was applied to improve the Kuz-Ram model's predictive capability for blast fragmentation. Traditional Kuz-Ram fragmentation predictions rely on an empirical rock factor (*Rf*) that requires calibration for site-specific geological conditions. However, this calibration is often heuristic and lacks an explicit functional representation of key blast parameters [10]. To address this limitation, a quadratic response surface model was developed to estimate the effective rock factor ($Rf_{effective}$) as a function of the blastability index *(BI)*. The quadratic polynomial equation used for this estimation is given in equation 6:

$$Rf_{effective}(BI) = \beta_0 + \beta_1 \times (BI) + \beta_2 \times (BI)^2 \quad (6)$$

where β_0, β_1, β_2 are regression coefficients obtained through least squares method.

The derived coefficients for the modified Kuz-Ram rock factor function are presented in equation 7:

$$Rf_{effective}(BI) = 0.0824 - 0.0050(BI) - 0.0001(BI)^2 \quad (7)$$

Incorporating the effective rock factor into the modified Kuz-Ram model, the overall model can be expressed as shown in equation 8:

$$X_{50} = [0.0824 - 0.005 \times BI - 0.0001 \times BI^2]\ Rf \times K^{-4/5} \times Q^{1/6} \times \left(\frac{115}{RWS}\right)^{19/20} \quad (8)$$

Equation 8 systematically integrates variations in the blastability index, enhancing the prediction of mean fragmentation and improving adaptability to different rock masses. By incorporating a response surface approach, the refined Kuz-Ram equation improves fragmentation predictions while maintaining interpretability. This enhancement ensures that site-specific blast parameters are effectively accounted for, minimising reliance on heuristic calibrations and making the model more applicable across diverse geological and operational conditions. The canonical Kuz-Ram formulations by Cunningham [10, 15-16] and the commonly cited modification by Gheibie et al. [18] as physically interpretable predictors was used. We do not re-estimate their parameters here; instead, they form the engineering baseline upon which our response-surface (RSM) correction operates. This choice follows published evidence that Kuz-Ram variants can exhibit systematic misfit without site-specific calibration [16,18].

a). Sampled images of the muck pile.

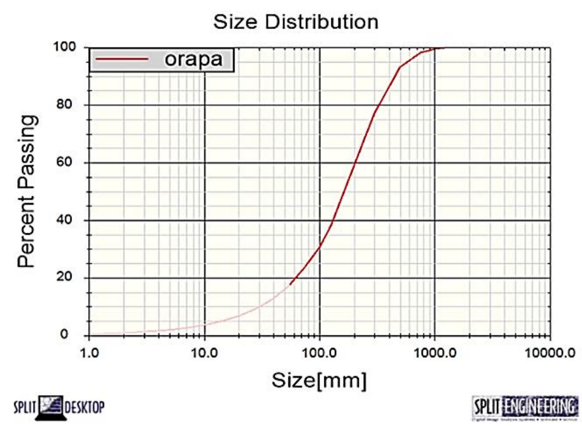

b) Particle size distribution curve.

Figure 4. Images of the muck pile and the resulting particle size distribution curve.

3. Results and discussions

Three key performance indices were employed to assess each predictive model's efficacy: root mean square error (RMSE), mean absolute error (MAE), and coefficient of determination (R^2). These metrics are defined by equations 9 to 11:

$$RMSE = \sqrt{\frac{1}{N}\sum_{i=1}^{N}(yi - yi')^2} \quad (9)$$

$$MAE = \frac{1}{n}\sum_{i=1}^{n}|yi - yi'| \quad (10)$$

$$R2 = \left[1 - \frac{\sum_{i=1}^{N}(yi - yi')}{\sum_{i=1}^{N}(yi - \bar{y}i)^2}\right]^2 \quad (11)$$

where n is the number of observations, y_i and y_i' are the measured and predicted values respectively of the i^{th} observation, and $\bar{y}i$ are the mean values.

Table 3 presents the performance comparison between the two models, demonstrating that the modified Kuz-Ram model outperforms the baseline model. The modified model achieves a higher R2 value of 57.9% and lower error metrics, with a mean absolute error (MAE) of 3.072 and a root mean square error (RMSE) of 5.7136. This represents a 12.2% improvement in accuracy compared to the baseline model.

Table 3. Model performance metrics.

Model	R2	MAE	RMSE
Kuz-Ram Model	0.457	4.976	7.1252
Modified Kuz-Ram Model	0.579	3.072	5.7136

The scatter plot in Figure 5b further illustrates the enhanced agreement between the measured and predicted mean fragmentation sizes for the modified Kuz-Ram model compared to the baseline Kuz-Ram model in Figure 5a. These results suggest that by incorporating the blastability index into the calculation of the rock factor, the modified model can more effectively capture the differences in rock mass properties. This adaptation allows for a better prediction of the degree of fragmentation, reflecting the influence of geological variations on blast outcomes. This underscores the significant influence of geological characteristics on blasting efficiency, highlighting the blastability index as a critical parameter. This finding corroborates earlier studies that reported significant prediction errors when applying unmodified Kuz-Ram equations to heterogeneous rock masses, underscoring the necessity of context-specific recalibration [12, 18].

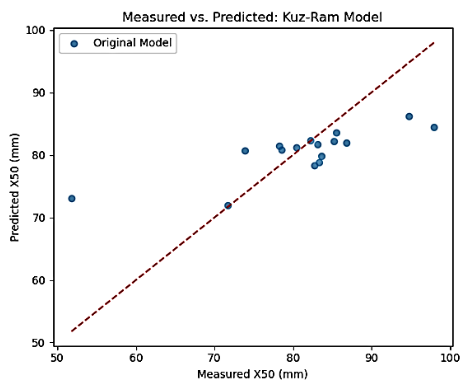

(a). Kuz-Ram model results.

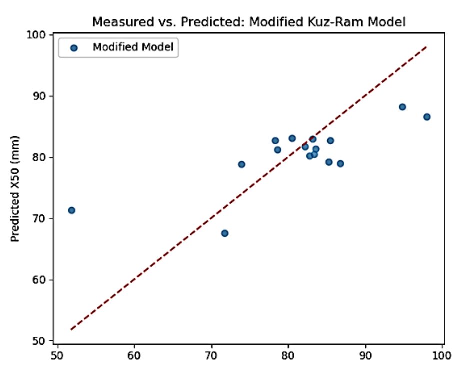

(b). Modified Kuz-Ram model results.

Figure 5. Measured vs. Predicted mean fragmentation by two models.

3.1. Application of the RSM-Modified Kuz-Ram model

Figure 6 (a & b) shows the 3D response surface model based on the modified Kuz-Ram model. From Figure 6a, it can be observed that an increase in the blastability index combined with a decrease in the powder factor leads to an optimised X_{50}, indicating that better blastability (typically associated with weaker rock) and lower powder factor lead to finer fragmentation. It also suggests that excessive powder factor does not always yield good fragmentation and that adjusting explosive energy relative to rock properties is critical in blast optimisation. Figure 6b shows that a moderate combination of charge and blastability index results in an optimal X_{50}, implying that extremely high or low values of these parameters may lead to suboptimal fragmentation. The response surface shows that there exists a balance in explosive energy and rock mass characteristics that maximises fragmentation efficiency.

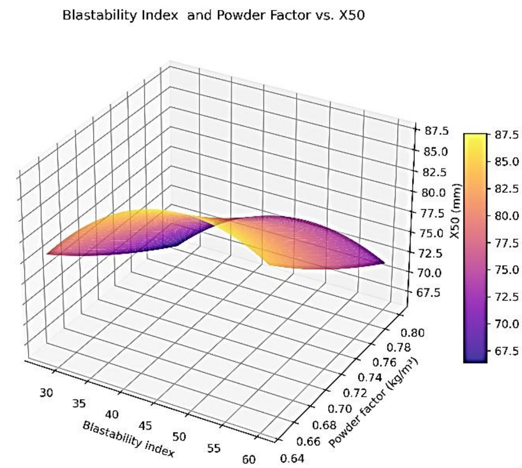

(a). BI and Pf vs. mean fragmentation.

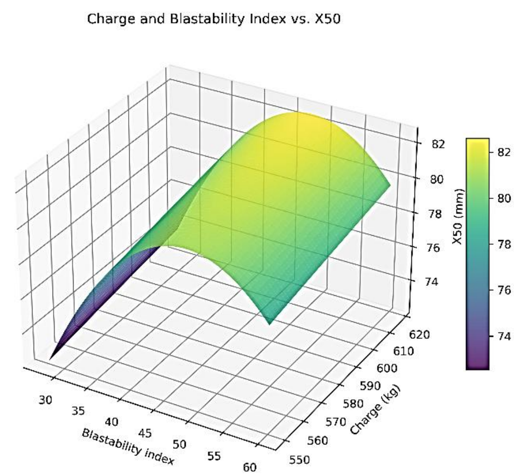

(b). BI and C vs. mean fragmentation.

Figure 6. 3D response surface plots of fragmentation prediction.

These analyses enable engineers to fine-tune blast parameters based on specific rock conditions to optimise fragmentation outcomes and to improve downstream processing efficiency. Unlike machine learning models, which act as black-box predictors, the response surface approach provides explicit mathematical relationships, making it more practical for blasting applications by allowing direct interpretation of parameter effects and interactions. These findings emphasise the importance of data-driven decision-making in blast design, ensuring that fragmentation is controlled while minimising excessive energy consumption. Figure 7 shows the relationship between blastability index and the effective rock factor. The observed values are represented by blue scatter points and the quadratic fitted response surface depicted by the red curve. The trend suggests a nonlinear relationship, where *Rf* initially increases with blastability index, it reaches a peak and then starts to decline slightly at BI values > 45. This indicates that as the blastability of rock improves, the effective rock factor follows an increasing trend up to a certain threshold, beyond which additional increases in blastability may not be proportionally related to the rock factor. Such behaviour could be attributed to variations in rock material properties, geotechnical conditions, or interactions between input parameters affecting fragmentation efficiency. The nonlinearity in the response suggests that a simple linear model may not sufficiently capture the relationship between BI and effective rock factor, making higher-order models more suitable for predictive analysis. Understanding this trend is crucial for optimising blast design, as it informs adjustments to explosives and blasting parameters to achieve the desired fragmentation while minimising any possible inefficiencies.

The integration of RSM into the Kuz-Ram framework significantly improved fragmentation prediction accuracy, as evidenced by the increase in R2 from 0.457 to 0.579 and the corresponding reductions in RMSE and MAE (Table 2). This 12.2% improvement demonstrates that explicitly modelling the nonlinear relationship between blastability index (BI) and rock factor enhances the adaptability of the Kuz-Ram model to heterogeneous rock masses such as kimberlite at Orapa Mine. These findings align with previous studies that emphasised the limitations of the baseline Kuz-Ram model in complex geological conditions but extend them by introducing a statistically rigorous method rather than heuristic recalibrations [12, 18].

A key insight from the response surface analysis (Figures 6 and 7) is that fragmentation outcomes are not linearly proportional to any single parameter but result from the combined effects of BI, powder factor, and charge. Specifically, increasing BI generally reduces mean fragment size due to more favourable rock mass characteristics such as, jointing, lower and compressive strength. However, the optimisation surface revealed a threshold beyond which additional increases in BI no longer yield proportional improvements, indicating a plateau effect likely related to geological variability. Similarly, while higher powder factors typically enhance fragmentation, the response surfaces show diminishing returns at excessive energy input, suggesting that overcharging can be inefficient and may lead to adverse effects such as flyrock, back-break, or excessive fines [8, 40].

Comparative analysis of the modified and baseline models further supports the significance of incorporating BI into rock factor calculations. Traditional rock factor estimation often overlooks geological heterogeneity, relying instead on empirical adjustments or average conditions [11, 16]. By contrast, the RSM-based approach captures site-specific variations in rock properties and provides a polynomial expression that can be readily recalibrated as new data are collected. This makes it particularly advantageous for operations like Orapa Mine, where kimberlite exhibits varying degrees of weathering, jointing, and density across different benches.

The practical implications of this refinement are substantial. Improved prediction of X_{50} allows engineers to design blasts that minimise oversize material, thereby reducing secondary breakage requirements and enhancing loading and hauling efficiency. Furthermore, by identifying the optimal combinations of BI, powder factor, and charge, operations can reduce explosive consumption without compromising fragmentation quality, supporting cost savings and sustainability objectives in large-scale open-pit mining. Despite these advantages, the study also has limitations. The dataset was limited to four static input parameters and did not account for dynamic factors such as initiation timing, inter-hole delays, and energy distribution patterns, which are known to influence fragmentation outcomes [38]. Additionally, while the model demonstrated improved predictive performance, further validation with independent datasets from different lithologies is required to confirm its broader applicability.

Future research should therefore extend this framework by incorporating timing parameters, burden-to-spacing ratios, and geotechnical indices derived from advanced rock mass classification systems. Integrating these factors could further enhance model robustness and provide a more comprehensive tool for blast design optimisation. Moreover, coupling the RSM-modified Kuz-Ram model with machine learning algorithms could enable hybrid approaches that retain interpretability while leveraging the predictive power of data-driven methods.

4. Conclusions

This study utilised blasting data from Orapa Diamond Mine to develop a refined Kuz-Ram model that integrates response surface methodology (RSM) for improved fragmentation prediction. By incorporating four key parameters, charge, powder factor, rock factor, and blastability index, the modified model captured nonlinear interactions between geological and design factors, achieving a 12.2% improvement in prediction accuracy compared to the baseline Kuz-Ram model. The model reached an R^2 of 0.579, reducing RMSE and MAE to 5.71 and 3.07, respectively, which represents a substantial improvement over the original model's performance. The response surface analysis further revealed that the optimal fragmentation (X_{50}) is achieved when higher blastability indices are combined with controlled powder factors, avoiding excessive energy input that leads to oversize or excessive fines. This balance provides clear guidance for field engineers to optimise blast design and improve downstream efficiency in loading, hauling, and crushing operations. The study was limited to static parameters from a single kimberlite deposit and did not consider dynamic factors such as timing or burden-to-spacing variations. Additionally, the model has not yet been validated on newly executed blasts; future work will involve applying the model to prospective field blasts to confirm its predictive reliability. Broader validation across diverse lithologies and integration of additional geotechnical and timing parameters are also recommended. Further improvements could involve hybridizing this RSM approach with machine learning methods and incorporating cost-benefit analyses to enhance both predictive performance and economic impact in mine planning.

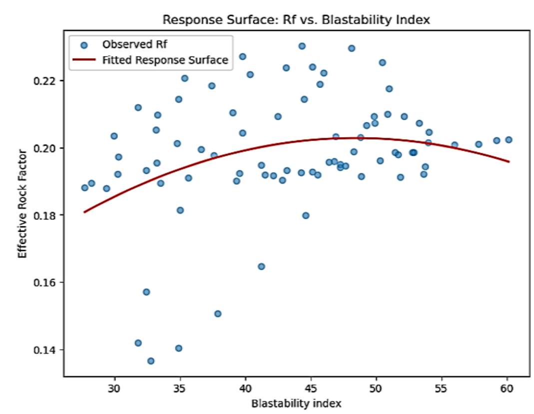

Figure 7. Response surface for effective rock factor against blastability index.

Conflict of Interest

The authors declare that they have no conflict of interest.

References

[1]. Ouchterlony, F. (2003). Influence of blasting on the size distribution and properties of muckpile fragments: a state-of-the-art review. MinFo Project P2000-10: Energy Optimisation in Comminution, 9 December, 21-27.

[2]. Shams, S., Monjezi, M., Majd, V.J. and Armaghani, D.J. (2015). Application of fuzzy inference system for prediction of rock fragmentation induced by blasting. Arab. J. Geosci., 8: 10819-10832.

[3]. Bamford, T., Esmaeili, K. and Schoellig, A.P. (2021). A deep learning approach for rock fragmentation analysis. Int. J. Rock Mech. Min. Sci., 145: 104839.

[4]. Kanchibotla, S.S., Valery, W. and Morrell, S. (1999). Modelling fines in blast fragmentation and its impact on crushing and grinding. Proc., Explo '99, 137-144.

[5]. Ghosh, R., Schunnesson, H. and Gustafson, A. (2022). Predicting rock fragmentation based on drill monitoring. J. S. Afr. Inst. Min. Metall., 122(3): 153-160.

[6]. Lilly, P.A. and Kecojevic, V. (2010). Improving safety in blasting

operations by controlling flyrock and ground vibration. Saf. Sci., 48(10): 1339-1345.

[7]. Cho, S.H., Nishi, M., Yamamoto, M. and Kaneko, K. (2003). Fragment size distribution in blasting. Mater. Trans., 44(5): 951-956.

[8]. Ouchterlony, F. (2005). The Swebrec function: linking fragmentation by blasting and crushing. Min. Technol. (Trans. Inst. Min. Metall. A), 114: A29-A44.

[9]. Kuznetsov, V.M. (1973). The mean diameter of the fragments formed by blasting rock. Sov. Min. Sci., 9: 144-148.

[10]. Cunningham, C.V.B. (1983). The Kuz-Ram model for prediction of fragmentation from blasting. Proc., 1st Int. Symp. on Rock Fragmentation by Blasting, Lulea, Sweden, 439-453.

[11]. Lilly, P.A. (1986). An empirical method of assessing rock mass blastability. Proc., Large Open Pit Mine Conf., Newman, 89-92.

[1]2. Tosun, A., Konak, G., Toprak, T., Karakus, D. and Onur, A.H. (2014). Development of the Kuz-Ram model to blasting in a limestone quarry. Arch. Min. Sci., 59(2): 477-488.

[13]. Lawal, A.I. (2021). A new modification to the Kuz-Ram model using the fragment size predicted by image analysis. Int. J. Rock Mech. Min. Sci., 138: 104595.

[14]. Monjezi, M., Rezaei, M. and Mohammadi, S.S. (2009). Environmental impact assessment of blasting operations in limestone mines using fuzzy logic. Int. J. Rock Mech. Min. Sci., 46(8): 1323-1330.

[15]. Cunningham, C.V.B. (1987). Fragmentation estimations and the Kuz-Ram model - four years on. Proc., 2nd Int. Symp. on Rock Fragmentation by Blasting, Keystone, CO, 23–26 August 1987, Society of Experimental Mechanics, Bethel, 475-487.

[16]. Cunningham, C.V.B. (2005). The Kuz-Ram fragmentation model - 20 years on. Proc., 3rd World Conf. on Explosives and Blasting, Brighton, UK, 13–16 September 2005, 201-210.

[17]. Wang, X., Zhang, Y. and Li, H. (2023). Simulation-based hybrid optimisation for blast design considering fragmentation and vibration control. Simul. Model. Pract. Theory, 130: 102844.

[18]. Gheibie, S., Aghababaei, H., Hoseinie, S.H. and Pourrahimian, Y. (2009). Modified Kuz-Ram fragmentation model and its use at the Sungun Copper Mine. Int. J. Rock Mech. Min. Sci., 46(6): 967-973.

[19]. Zhou, Z., Chen, C., Cai, X. and Wang, P. (2024a). Blastability evaluation for rock mass: review and new tendency. Bull. Eng. Geol. Environ., 83(12): 517.

[20]. Chatziangelou, M. and Christaras, B. (2017). A New Development of BQS (Blastability Quality System) for Closely Spaced Formations. J. Geol. Res. Eng., 5(1): 1-12.

[21]. Navarro, J., Kuchar, S., Bordes, M., et al. (2021). Blastability and Ore Grade Assessment from Drill Monitoring for Open Pit Applications. Roc. Mech. Roc. Eng., 54: 4133-4153.

[22]. Segaetsho, G. and Zvarivadza, T. (2019). Application of rock mass classification and Blastability Index for the improvement of wall control: a hard-rock mining case study. J. S. Afr. Inst. Min. Metall., 119(1): 31-38.

[23]. Shi, X.Z., Zhou, J., Wu, B.B., Huang, D. and Wei, W. (2012). Support vector machines approach to mean particle size of rock fragmentation due to bench blasting prediction. Trans. Nonferrous Met. Soc. China, 22(2): 432-441.

[24]. Fang, Q., Nguyen, H., Bui, X.-N., Nguyen-Thoi, T. and Zhou, J. (2020). Modeling of rock fragmentation by firefly optimization algorithm and boosted generalized additive model. Neural Comput. Appl., 33: 3503-3519.

[25]. Dumakor-Dupey, N.K., Arya, S. and Jha, A. (2021). Advances in blast-induced impact prediction - a review of machine learning applications. Minerals, 11(6): 601.

[26]. Amoako, R., Jha, A. and Zhong, S. (2022). Rock fragmentation prediction using an artificial neural network and support vector regression hybrid approach. Mining, 2(2): 233-247.

[27]. Huang, J., Asteris, P.G., Khajeh Pasha, S.M., Mohammed, A.S. and Hasanipanah, M. (2022). A new auto-tuning model for predicting the rock fragmentation: a cat swarm optimization algorithm. Eng. Comput., 38: 2209-2220.

[28]. Zhou, J., Zhang, Y. and Qiu, Y. (2024b). State-of-the-art review of machine learning and optimization algorithms applications in environmental effects of blasting. Artif. Intell. Rev., 57, Article 5: 29-33.

[29]. Samui, P. and Kothari, D.P. (2009). Application of neural networks and expert systems in predicting and optimising blasting outcomes. Expert Syst. Appl., 36(3): 5980-5986.

[30]. Ghoraba, S., Zolfaghari, A. and Asadi, A. (2017). Hybrid intelligent optimisation techniques for rock engineering problems: a review and new approach. Eng. Comput., 33(4): 899-912.

[31]. Enayatollahi, I., Bazzazi, A.A. and Asadi, A. (2014). Comparison between neural networks and multiple regression analysis to predict rock fragmentation in open pit mines. Rock Mech. Rock Eng., 47(3): 799-807.

[32]. Rudin, C. (2019). Stop explaining black box machine learning models for high stakes decisions and use interpretable models instead. Nat. Mach. Intell., 1(5): 206-215.

[33]. Box, G.E.P. and Wilson, K.B. (1951). On the experimental attainment of optimum conditions. J. R. Stat. Soc. Ser. B (Methodological), 13(1): 1-45.

[34]. Myers, R.H., Montgomery, D.C. and Anderson-Cook, C.M. (2016). Response Surface Methodology: Process and Product Optimization Using Designed Experiments, 4th ed., John Wiley & Sons, Hoboken, NJ, 390 P.

[35]. Montgomery, D.C. (2017). Design and Analysis of Experiments, 9th ed., John Wiley & Sons, Hoboken, NJ, 558 P.

[36]. Gernon, T.M., Field, M., Sparks, R.S.J., Brown, R.J., Fontana, G. and Mac Niocaill, C. (2008). Pyroclastic flow deposits from a kimberlite eruption: Orapa South Crater, Republic of Botswana. 9th International Kimberlite Conference Extended Abstracts, No. 9IKC-A-00177.

[37]. Bhandari, S. (1997). Engineering Rock Blasting Operations, A.A. Balkema, Rotterdam, Netherlands, 206 P.

[38]. Roy, M.P., Paswan, R.K., Sarim, M.D., Kumar, S., Jha, R.R. and Singh, P.K. (2016). Rock fragmentation by blasting - a review. J. Mines, Met. Fuels, 64(9).

[39]. Kulula, M.I., Nashongo, M.N. and Akande, J.M. (2017). Influence of blasting parameters and density of rocks on blast performance at Tschudi Mine, Tsumeb, Namibia. J. Miner. Mater. Charact. Eng., 5(6): 339.

[40]. Kanchibotla, S. S., Valery, W., & Morrell, S. (1999). Modelling fines in blast fragmentation and its impact on crushing and grinding. In Explo-99: A Conference on Rock Breaking, Kalgoorlie, WA, November 1999. Australasian Institute of Mining and Metallurgy, pp. 137–144.